

# Evaluating an image based multi-angle measurement setup using different reflection models

Aditya Sole, Ivar Farup, and Peter Nussbaum;  
The Norwegian University of Science and Technology, Gjøvik, Norway,

## Abstract

Image based measurement setups are widely used for multi-directional reflectance measurements of materials. Different reflection models are used to estimate the material reflectance.

In this paper we use two commonly known simple reflection models to evaluate an image based measurement setup proposed in our previous studies. Sample material is measured at multiple incident and viewing directions using the setup. The captured data is divided into training and test set to evaluate the setup. Two reflection models are trained using the training dataset. To evaluate the measurement setup, one of the sample materials is measured at few incident and viewing directions using a light source and a Tele-Spectro-Radiometer (TSR). This measured data is then compared with the reflectance estimated by the two reflection models.

Results shows that image based multi-directional reflectance measurements can be performed using measurement setup proposed in our previous work. The data captured using the setup can be used to fit different reflections models for the sample materials used in this setup.

## Introduction

Image based instruments that are relatively cheap and fast, are being increasingly used in multi-angle reflectance measurements of the material [1, 2, 3]. The multi-angle data captured can be further processed (for example to estimate the material BRDF). Where the need is to acquire fast and cheap measurements, image based instruments can be a good alternative compared to the expensive, time consuming, but precise instruments (like Goniospectrometers). These measurements can then be used to train reflection models to calculate the BRDF and simulate or reproduce the material appearance. A number of reflection models are proposed till now which mainly aim towards fulfilling the needs of the computer graphics field to simulate material appearance in a given scene/situation. One of the main aims of the computer graphics field is to accurately measure the appearance of materials and simulate/reproduce synthetically the real object using simple methods/techniques [4]. A Bidirectional Reflection Distribution Function (BRDF) is a distribution function that describes the surface reflectance properties of opaque and homogeneous materials [5] as given in Equation (1).

$$f_{BRDF}(\theta_i, \phi_i; \theta_r, \phi_r, \lambda) = \frac{dL_r(\theta_i, \phi_i, \theta_r, \phi_r, E_i)}{dE_i(\theta_i, \phi_r)} \quad (1)$$

Here,  $i$  and  $r$  denote incidence and reflection respectively.  $\theta$  and  $\phi$  together indicate the direction,  $E_i$  is incident irradiance,  $L_r$  is radiance and  $d$  is the differential. Guarnera [4] presented an overview

of the BRDF models used to represent surface/material reflection characteristics. As discussed in [4], BRDF models can be classified into Physically-based models and Phenomenological models. Physically-based models are based on physics and optics and are described using micro-facets of varying size and orientations. One of the very well known and widely used physical models is the Cook-Torrance [6] model. Phenomenological models are approximations of the reflectance data using measured data and fitting of the same using analytical models. Some of the commonly known phenomenological models are the Phong [7], Ward [8], Lafortune [9], etc.

In our previous studies [3] we presented a measurement setup which can perform multi-angle reflectance measurements of homogenous, flexible materials in a fast and relatively cheap way. In this setup, we mount the flexible sample onto a cylinder of known radius and measure using a RGB camera [10, 3]. The captured RGB data is converted into the colorimetric space CIEXYZ using the conversion matrix  $\hat{M}$ . Matrix  $\hat{M}$  is derived using the camera spectral sensitivity (measured using a monochromator) and the CIE 2° colour matching functions by minimising the error using least square technique [11]. This data can be used further as training data to train different reflection models (like Cook-torrance or Ward model) to estimate the sample BRDF and simulate the material appearance.

The objectives of the work presented in this paper are:

- to estimate the surface reflectance properties of the sample materials used in the experimental setup using the image based multi-angle measurement setup proposed in previous studies [3],
- to train different reflection models using the colorimetric data captured with the image based multi-angle measurement setup and evaluate the setup against measurements obtained using a TSR,
- test the trained reflection models to predict the sample material reflectance at different illumination and viewing directions.

## Background

In order to evaluate the measurement setup we used 2 reflections models; Cook-Torrance (hereby referred as CT in this paper) and Ward to fit the measurement data obtained in the measurement setup by using the RGB camera [3]. The trained model parameters were then used to estimate the BRDF measurement at different incident and viewing directions. CT model is a physical model that describes the intensity and spectral composition of the light reflected from the object/material. CT model as described in

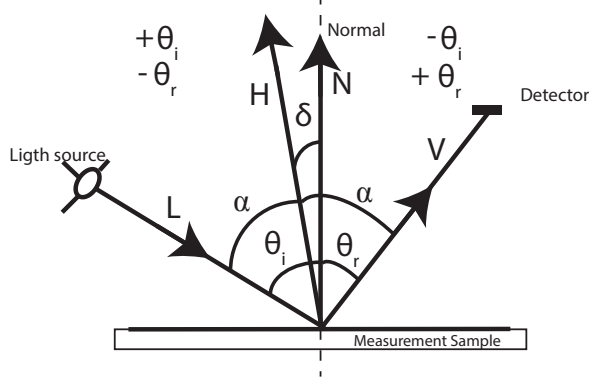


Figure 1. Angles and vectors used in reflection equations.

[6] is given in Equation (2).

$$I_r = I_{ia}R_a + \sum_l I_{il}(\mathbf{n} \cdot \mathbf{l})\omega_l(sR_s + dR_d) \quad (2)$$

Where,  $I_r$  is the total reflected intensity reaching the viewer,  $I_{ia}$  is the ambient light intensity,  $R_a$  is the ambient reflection component,  $I_{il}$  is the incident light intensity for incident light  $\mathbf{l}$ ,  $\mathbf{n}$  is the normal vector as the given pixel point ( $P$ ),  $\mathbf{l}$  is the incident light vector,  $\omega_l$  is the incident light solid angle,  $s$  and  $d$  are the specular and diffuse component co-efficients dependent on the material being simulated/reproduced,  $R_s$  and  $R_d$  are the specular and diffuse component of the model. The ambient  $R_a$  and diffuse  $R_d$  component of the model reflect light equally in all directions and therefore are independent of the location of the observation, whereas, the specular  $R_s$  component is dependent on the location of observation. For the specular component  $R_s$ , the angular spread is described assuming that the surface consist of microfacets, whose normal is in the  $\mathbf{h}$  direction and contributes in the specular component of reflection. Vector  $\mathbf{h}$  is the half angle vector between the viewing vector  $\mathbf{v}$  and incident light vector  $\mathbf{l}$  such that  $\mathbf{l} \cdot \mathbf{h} = \mathbf{v} \cdot \mathbf{h}$ . The specular component is given as

$$R_s = \frac{FDG}{\pi(\mathbf{n} \cdot \mathbf{l})(\mathbf{n} \cdot \mathbf{v})} \quad (3)$$

where,  $F$  is the Fresnel term that describes how light is reflected from each microfacet.  $G$  is the geometrical attenuation factor accounting for the shadow and masking and  $D$  is the Beckmann distribution.  $\mathbf{n}$  is the vector normal at the given pixel point ( $P$ ),  $\mathbf{v}$  is the viewing vector and  $\mathbf{l}$  is the illumination vector.  $G$  and  $D$  are given as

$$G = \min \left\{ 1, \frac{2(\mathbf{n} \cdot \mathbf{h})(\mathbf{n} \cdot \mathbf{v})}{(\mathbf{v} \cdot \mathbf{h})}, \frac{2(\mathbf{n} \cdot \mathbf{h})(\mathbf{n} \cdot \mathbf{l})}{(\mathbf{v} \cdot \mathbf{h})} \right\} \quad (4)$$

$$D = \frac{1}{m^2 \cos^4 \alpha} e^{-[(\tan \delta)/m]^2}$$

where  $\alpha$  is the angle between  $\mathbf{n}$  and  $\mathbf{h}$  (refer Figure 1),  $m$  is the root mean square slope of the facet in the material (or roughness co-efficient) and  $\mathbf{h}$  is the half angle vector between  $\mathbf{v}$  and  $\mathbf{l}$ .

Ward model [8] is a phenomenological model with the aim to fit measured reflectance data with a simple empirical formula. This model represents both isotropic and anisotropic reflection and

uses a gaussian distribution for the specular peaks. As the samples used in this work are isotropic samples we use the isotropic Ward model. The isotropic Ward model is given as

$$\rho_{bd_{iso}}(\theta_i, \phi_i; \theta_r, \phi_r) = \frac{\rho_d}{\pi} + \frac{\rho_s}{\sqrt{\cos \theta_i \cos \theta_r}} \frac{e^{[-\tan^2 \delta / \alpha^2]}}{4\pi\alpha^2} \quad (5)$$

here  $\rho_{bd_{iso}}$  is the bidirectional reflectance distribution for the given isotropic sample material,  $\rho_d$  is the diffuse reflectance,  $\rho_s$  is the specular reflectance,  $\delta$  is the angle between vectors  $\hat{n}$  and  $\hat{h}$  as shown in Figure 1,  $\alpha$  is the standard deviation (RMS) of the surface slope and  $1/4\pi\alpha^2$  is the normalisation factor.

## Method

### Sample measurement

Wax based inks printed on a matt coated white plotting paper were used as test sample material to capture using the image based multi-angle reflectance measurements. We used the OCE Color-Wave 600 to print 7 different colour samples on matt coated white plotting paper. These samples were measured using the measurement setup [3] at 10 different illumination directions ( $\theta_L = 5^\circ, 10^\circ, 15^\circ, 18^\circ, 20^\circ, 22^\circ, 25^\circ, 28^\circ, 30^\circ$ , and  $35^\circ$ ). A tungsten point light source was used to illuminate the samples and Nikon D200 DSLR camera as measurement sensor. Figure 2 shows the captured image of the sample at  $\theta_L = 15^\circ$ . Spectralon tile was used as reference white in the scene. The incident ( $\theta_i$ ) and reflection ( $\theta_r$ ) angles at given pixel points ( $P$ ) were calculated for all the illumination directions ( $\theta_L$ ). Raw images of the samples were captured. No white balance or gamma corrections are performed on the captured RGB data. The captured R, G and B intensities are transformed into CIEXYZ colour space using the transformation matrix  $\hat{M}$  derived using the camera spectral sensitivity (measured using a monochromator) and the CIE  $2^\circ$  colour matching functions by minimising the error using least square technique [11].

### Training of the BRDF models

As the print samples are reproduced from wax inks, as can be seen in the captured image (refer Figure 2), the samples show some specularly but overall are diffuse. We train two BRDF models (CT and Ward) using the camera measurements of these samples. These samples are measured at 10 different incident light directions ( $\theta_L$ ). Figure 3 and 4 show plots of the CIE Y for the corresponding viewing angles ( $\theta_r$ ) for the samples Cyan and Pantone 10309C measured at  $\theta_L = 25^\circ$  and  $28^\circ$ . To train the 2 models we use measurement data (hereby referred as training dataset) of 5 of these 10 incident light directions (particularly  $5^\circ, 15^\circ, 20^\circ, 25^\circ$  and  $30^\circ$ ). Figure 1 shows the sign convention followed for the measurement angles in this paper. The same sign convention is followed in the image based multi-angle measurement setup and the TSR measurements performed.

### Cook-Torrance model

Assuming that the samples are homogeneous, uniform and non-flourescent, to train the CT model, we insert the measurement setup parameters in Equation (2). The camera colorimetric output



Figure 2. Captured image of the samples.

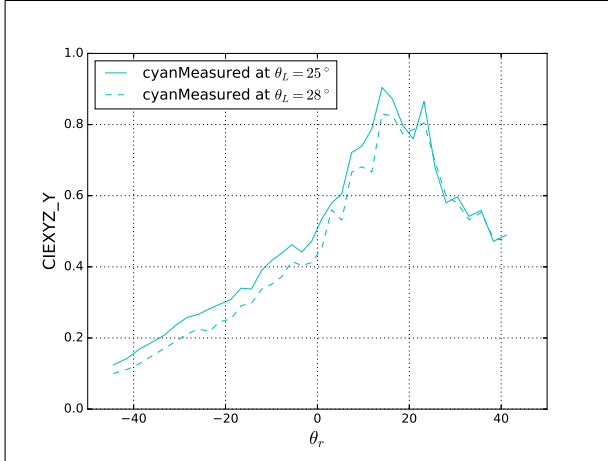


Figure 3. CIEXYZ Y value, Cyan sample.

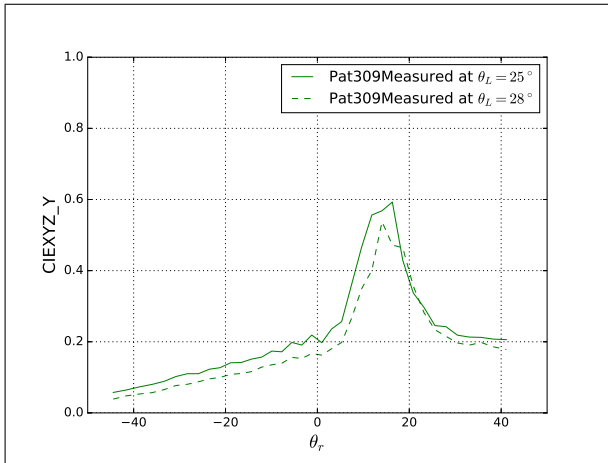


Figure 4. CIEXYZ Y value, Pantone 10309C sample.

$I_{(x,y,z)}$  at pixel points ( $P$ ) will be,

$$I_P = \begin{bmatrix} I_{P_x} \\ I_{P_y} \\ I_{P_z} \end{bmatrix} = I_{ia}R_a + I_i(\mathbf{n} \cdot \mathbf{l})(sR_s + dR_d) \quad (6)$$

To simplify the optimisation of the CT model, we use  $s + d = 1$ . Therefore,

$$I_P = \begin{bmatrix} I_{P_x} \\ I_{P_y} \\ I_{P_z} \end{bmatrix} = I_{ia}R_a + I_i \cos \theta_i \left( k_s R_s + (1 - k_s) \begin{bmatrix} R_{dx} \\ R_{dy} \\ R_{dz} \end{bmatrix} \right) \quad (7)$$

Where,  $R_s$  is as defined in Equation (3),  $F$  is assumed as 1,  $D$  and  $G$  are as defined in Equations (4),  $I_{ia}R_a$  = ambient light (assumed as zero as the measurements are performed in dark conditions),  $I_i$  = incident light intensity,  $\theta_i$  = angle between the incident light direction and normal to the sample surface,  $\theta_r$  = angle between the viewing direction and normal to the sample surface,  $k_s$  = specular coefficients of the sample material,  $R_s$  = specular reflectance component,  $R_{dx,y,z}$  = spectral diffuse reflectance component,  $\delta = \mathbf{n} \cdot \mathbf{h} = \cos((\theta_i - \theta_r)/2)$  at the given pixel point ( $P$ ) in the used measurement setup,  $\mathbf{n} \cdot \mathbf{l} = \cos \theta_i$ ,  $\mathbf{n} \cdot \mathbf{v} = \cos \theta_r$ . As the area on the sample measured by the pixel being very small we absorb the solid angle  $\omega_l$  term in the coefficients  $K_s$  and  $R_{dx,y,z}$ .

### Ward model

As the training dataset is the colorimetric data obtained from camera output in terms of RGB intensities, we train the Ward model using the intensity measurements rather than as reflectance. Also the measurements being planner, angle ( $\phi$ ) can be ignored. Inserting the measurement setup parameters in Equation (5)

$$I_P(\theta_i; \theta_r) = \begin{bmatrix} I_{dx} \\ I_{dy} \\ I_{dz} \end{bmatrix} = I_i \cos \theta_i \left( \begin{bmatrix} R_{dx} \\ R_{dy} \\ R_{dz} \end{bmatrix} \frac{1}{\pi} + \frac{k_s}{\sqrt{\cos \theta_i \cos \theta_r}} \frac{e^{-\tan^2 \delta / m^2}}{4\pi m^2} \right) \quad (8)$$

where,  $I_i$  = incident light intensity,  $\theta_i$  and  $\theta_r$  as explained in the CT model,  $k_s$  = specular coefficients of the sample material,  $R_{dx,y,z}$  = spectral diffuse reflectance component,  $\delta = \cos((\theta_i - \theta_r)/2)$  at the given pixel point ( $P$ ) in the used measurement setup.

Reflection coefficients  $k_s$ ,  $R_{dx,y,z}$  and  $m$  are fitted and optimised using the training dataset. Nelder-Mead down-hill simplex algorithm [12] was used to optimise the coefficients using the  $\Delta E_{00}$  colorimetric difference as the error function. In order to calculate the  $\Delta E_{00}$  colorimetric difference, the CIEXYZ values were converted to CIELAB colour space using the same point light source that was used in the image based multi-angle measurement setup. The spectralon tile was measured using a Minolta CS1000 TSR for a given incident light directions. Assuming the spectralon tile as a perfect diffuser, these measurements were then used as the reference white in the CIELAB calculations. Table 1 provides the optimized co-efficient obtained for the 7 samples using both the models.

### Physical measurements using a TSR

To validate the image based multi-angle measurement setup against physical measurements (e.g. performed using gonio-

multiangle measurement setup using spectrometers), we measured one of the sample material (Cyan) using the Minolta CS1000 TSR at 4 different viewing directions ( $\theta_r$ ) for a given incident direction ( $\theta_i$ ). The cyan sample is measured at  $\theta_i = 40^\circ$  and  $\theta_r = -10^\circ, 0^\circ, 10^\circ$  and,  $30^\circ$ . Spectralon tile was measured along with the patch to normalise the radiance measurements and to calculate the spectral reflectance. The obtained spectral reflectances were converted to CIEXYZ colour space using the point light source (used in the image based multi-angle measurement setup) as the light source and transformed colour matching functions  $\hat{C}$  obtained using the matrix  $\hat{M}$  and the CIE  $2^\circ$  colour matching functions as derived in [11]. The obtained CIE Y value was then compared with the CIE Y value estimated using the trained CT and Ward model for the same incident and viewing directions. To estimate the CIEXYZ value using the BRDF models, we used the co-efficients  $R_{dx}, R_{dy}, R_{dz}, k_s$  and,  $m$  (refer Table 1) that are optimised using the camera measured training dataset. These co-efficients are implemented in Equations (7) and (8) for  $\theta_i = 40^\circ$  and  $\theta_r = -10^\circ, 0^\circ, 10^\circ$  and,  $30^\circ$ .

**Table 1: Coefficients for the 7 samples optimised using the CT and Ward model**

Material	$R_{dx}$	$R_{dy}$	$R_{dz}$	$k_s$	$m$
<i>CT model</i>					
Munsell white	1.175	1.131	2.215	0.042	0.393
Red	0.303	0.229	0.112	0.029	0.119
Cyan	0.517	0.519	1.465	0.068	0.230
Pantone 10309C	0.181	0.256	0.304	0.029	0.133
Magenta	0.499	0.374	0.651	0.079	0.222
Pantone 10213C	0.428	0.407	0.508	0.0	0.759
Pantone 10153C	0.426	0.324	0.219	0.095	0.252
<i>Ward model</i>					
Munsell white	1.508	1.451	3.5	0.663	0.45
Red	0.537	0.351	0.251	0.061	0.122
Cyan	0.951	1.022	2.756	0.163	0.249
Pantone 10309C	0.377	0.514	0.579	0.061	0.134
Magenta	0.864	0.596	1.286	0.174	0.225
Pantone 10213C	0.265	0.188	0.607	0.085	0.143
Pantone 10153C	0.817	0.591	0.561	0.119	0.197

## Results

We measured 7 sample materials at 10 different illumination directions ( $\theta_L$ ). We used the measurement data captured at 5 illumination directions as training data set to train the two models. In order to test the performance of the trained models we use the measured data from the remaining 5 illumination directions (particularly  $10^\circ, 18^\circ, 22^\circ, 28^\circ$  and  $35^\circ$  hereby referred to as test dataset) and compared the data estimated by the trained models at these illumination directions.

We use the  $\Delta E_{00}$  colorimetric difference [13] to compare the estimated and measured data. Table 2 shows the average, maximum and minimum colorimetric difference  $\Delta E_{00}$  obtained using the test dataset, between the camera measurements and the estimated data for all the samples. Figure 5 shows the histogram plot for the colorimetric difference calculated between the measured and estimated CIEXYZ values for the training dataset of all the

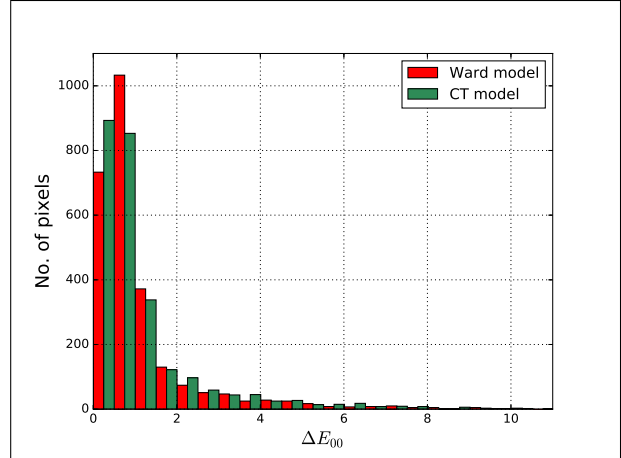


**Figure 5.**  $\Delta E_{00}$  histogram calculated for all the samples measured and estimated at the test dataset illumination angles using CT and Ward model.

samples. The average  $\Delta E_{00}$  obtained using the Ward model is 1.14 while with CT model is 1.17 with maximum number within the range of 0 to 2.0. From the histogram plot it can be observed that both the models perform well with the image based measurement setup for the samples used in this paper.

**Table 2: Colorimetric difference ( $\Delta E_{00}$ ) between camera measured data and data estimated data using CT and Ward model for all the samples**

Material	Avg. $\Delta E_{00}$	Max. $\Delta E_{00}$	Min. $\Delta E_{00}$
<i>CT model</i>			
Munsell white	0.61	3.37	0.06
Red	1.22	9.41	0.03
Cyan	0.91	3.65	0.11
Pantone 10309C	1.11	9.10	0.03
Magenta	1.45	7.47	0.07
Pantone 10213C	1.14	8.76	0.15
Pantone 10153C	1.75	10.86	0.14
<i>Ward model</i>			
Munsell white	0.75	2.16	0.11
Red	1.14	9.61	0.07
Cyan	0.91	3.66	0.12
Pantone 10309C	1.06	9.32	0.02
Magenta	1.44	8.18	0.04
Pantone 10213C	0.99	8.06	0.06
Pantone 10153C	1.69	11.63	0.07

For discussions in this paper, we look at two samples (Cyan and Pantone 10309C) out of these 7 samples measured at one illumination angle (at  $\theta_L = 28^\circ$ ) from the test dataset. Figure 6 and 7 show the plots for the Cyan and Pantone 10309C sample, measured and estimated CIE Y data, using these two models for  $\theta_L = 28^\circ$ . From the plots it can be observed that both the models work well with the measurement data captured using this setup. In order to evaluate the models colorimetrically, we calculate the  $\Delta E_{00}$  between the measured data and the estimated data for all the samples. For the viewing range of  $-40^\circ$  to  $+40^\circ$  where

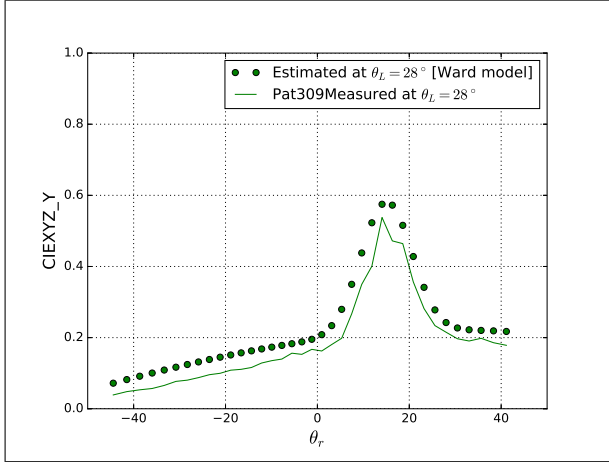


**Figure 6.** CIE XYZ Y value, Pantone 10309C sample, measured and estimated at  $\theta_L = 28^\circ$  using Ward model.

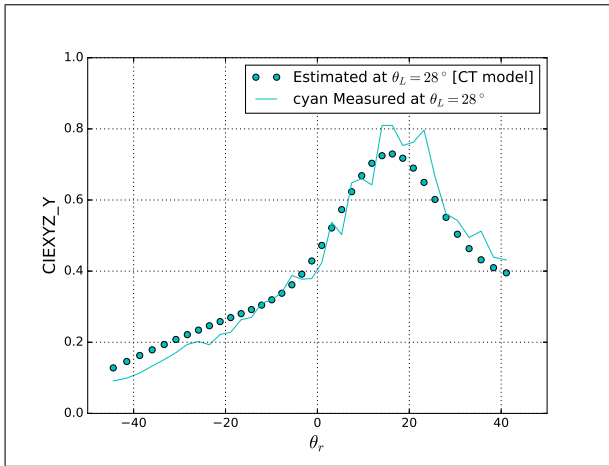


**Figure 7.** CIE XYZ Y value, Cyan sample, measured and estimated at  $\theta_L = 28^\circ$  using CT model.

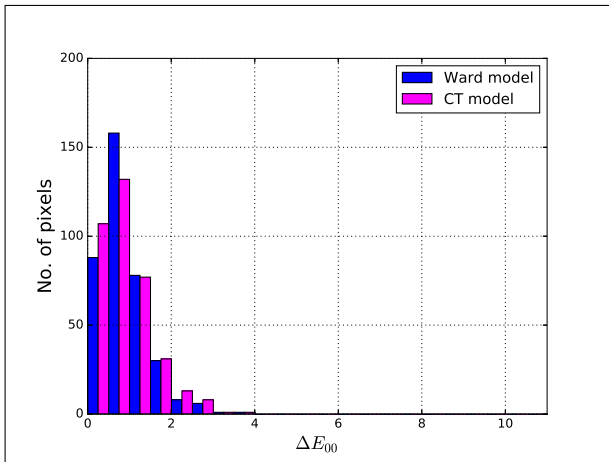


**Figure 8.**  $\Delta E_{00}$  histogram calculated for the Cyan sample CIE XYZ values, measured and estimated at the test dataset illumination angles using CT and Ward model.

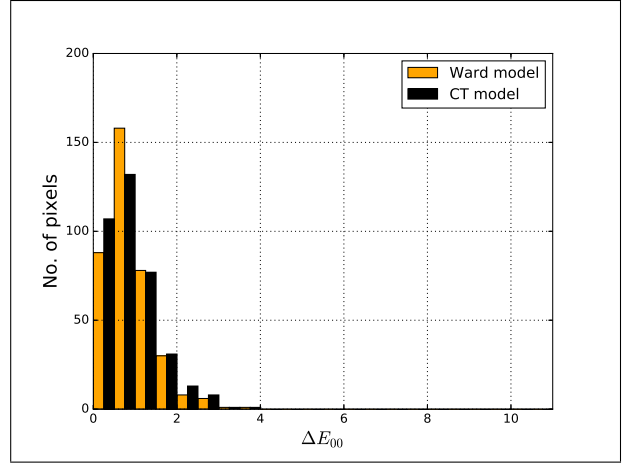


**Figure 9.**  $\Delta E_{00}$  histogram calculated for Pantone 10309C sample CIE XYZ values, measured and estimated at the test dataset illumination angles using CT and Ward model.

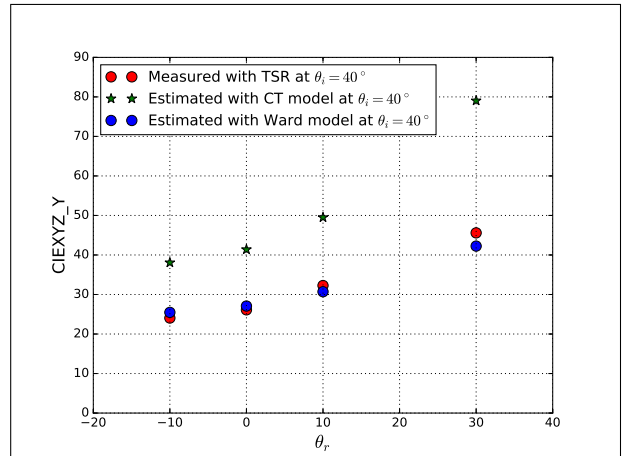


**Figure 10.** CIE Y values measured using TSR and estimated using the trained CT and Ward model.

the camera sensor is normal to the sample at  $\theta_r = 0^\circ$ , the colorimetric difference obtained shows that we can expect an ok fit using both the models. Figure 8 and 9 show the histogram plots for the colorimetric difference  $\Delta E_{00}$  between the measured and CT/Ward model estimated CIE Y values for the Cyan and Pantone 10309C sample. The trained models were compared with the physical measurements performed using the manual gonio-setup. Figure 10 shows the plots for the measured CIE Y data (using the TSR setup) and the estimated CIE Y data (using both the trained models) for the Cyan sample at  $\theta_i = 40^\circ$  and the viewing directions at which the physical measurements were performed.

## Discussions

In this paper we used two BRDF models to evaluate an image based multi-angle measurement setup. In total 7 samples were measured using the image based setup at 10 different illumination directions ( $\theta_L$ ). The samples are print samples of process and spot colours commonly used in package print industry. Wax based inks were used as they show some specularly and can also be processed further to reproduce 2.5D or 3D prints/objects. As

the selected samples showed some specularity but overall were diffuse, we used CT and Ward model. Both the models are simple and easy to implement for the type of samples used in this paper.

Specular and diffuse reflection coefficients along with the roughness coefficient were optimised for both the models using the training dataset. The  $\Delta E_{00}$  obtained between the test dataset and the estimated values shows that the error can perhaps be reduced further with 1) more careful geometrical and colorimetric calibration of the measurement setup, 2) using optimised illumination direction ( $\theta_L$ ) to train the BRDF models (either increasing the measurement data of reducing to the minimum possible illumination directions that will be sufficient to train the models). The histogram plots for the  $\Delta E_{00}$  obtained for the complete test dataset gives an understanding that the data captured using the image based measurement setup can, 1) be used to train different BRDF models, 2) estimate the colorimetric output of the material for simulation/reproduction purposes. Measurement data acquired from 5 out of the 10 illumination directions ( $\theta_L$ ) was used as training data set to train both the models and the remaining were used to test the performance of the models. The measured data was divided in half for training and testing purposes. There was no specific reason to choose measurement data from 5 angles as training dataset and the remaining as test dataset.

One sample (Cyan) was measured using a TSR at 4 different viewing directions for a given incident light direction. Using the optimised coefficients for the Cyan sample, the CIE Y value was estimated at the incident and viewing directions used in the TSR measurements. These estimated CIE Y values were compared with the TSR measurements. Looking at the plots (referring to Figure 10) we can see that the  $\Delta Y$  between the measurements (TSR) and the estimated CIE Y value follow the curvature/slope but increases for the last measurement at  $\theta_r = 30^\circ$ . This can also be observed in the ratio between  $\Delta Y$  and the *CIEY* value. One possible reason for this error could be that we have trained the CT model with measurement data obtained from the image based setup which uses a point light source to illuminate a curved sample. So the measurements obtained have varying illumination and viewing directions for the given pixel points. If we translate the TSR measurement angles to the image based measurement domain, we see that it corresponds to grazing angles in the image based measurement setup with a very low CIE Y corresponding value used to train the model. This also corresponds well with the TSR measurements which has a low CIE Y value at these angles. Another point to note is that the physical measurements performed using the TSR are not very accurate with respect to the incident and viewing direction angles.

## Conclusion

Looking at the results obtained, we can conclude that both the models perform satisfactorily using the measurement data captured using the image based multi-angle measurement setup. The CIE Y values estimated using the Ward model performed well compared to the CT model in terms of the colorimetric difference  $\Delta E_{00}$  obtained. The Ward model also estimates the data very well compared to the TSR measurements.

## Future work

As part of the future work it would be important to evaluate the image based measurement setup with gonio-measurements

obtained from a gonio-spectrometer setup or multi-angle instruments, where more precise angular measurements can be performed. It would also be important to evaluate the optimal measurement data (training dataset) that can be used to train the models. With respect to the image based measurement setup, using only 1 incident illumination angle ( $\theta_L$ ) would be ideal to train different reflection models.

## Acknowledgments

We would like to thank and acknowledge the support of Senior researcher Shoji Tominaga from Chiba University, Post Doctoral Researcher Jean-Baptiste Thomas, Giuseppe Claudio Guarnera, Thomas Simon and Tomas Majtner at the Norwegian Colour and Visual Computing Laboratory in discussions and suggestions regarding the experimental work and structure of this paper.

This work was supported by the MUVApp project N-250293, funded by the Research Council of Norway.

## References

- [1] J. Rong Lu, J. Koenderink, and A. M. L. Kappers, "Optical properties (bidirectional reflection distribution functions) of velvet," *Applied Optics*, vol. 37, pp. 5974 – 5984, September 1998.
- [2] S. R. Marschner, S. H. Westin, E. P. F. Lafortune, K. E. Torrance, and D. P. Greenberg, "Image-based brdf measurement including human skin," in *10th Eurographics Workshop on Rendering*, pp. 139 – 152, 1999.
- [3] A. S. Sole, I. Farup, and S. Tominaga, "An image-based multi-directional reflectance measurement setup for flexible objects," in *Measuring, Modeling and Reproducing Material Appearance 2015* (M. V. O. Segovia, P. Urban, and F. H. Imai, eds.), vol. SPIE 9398, pp. 93980J – 93980J–11, Proceedings of SPIE-IS& T Electronic Imaging, 2015.
- [4] D. Guarnera, G. Guarnera, A. Ghosh, C. Denk, and M. Glencross, "Brdf representation and acquisition," *Computer Graphics Forum*, vol. 35, no. 2, pp. 625–650, 2016.
- [5] F. E. Nicodemus, J. Richmond, J. J. Hsia, I. W. Ginsberg, and T. Limperis, "Geometrical considerations and nomenclature for reflectance." National Bureau of Standards, 1977.
- [6] R. L. Cook and K. E. Torrance, "A reflectance model for computer graphics," *ACM Trans. Graph.*, vol. 1, pp. 7–24, Jan. 1982.
- [7] B. T. Phong, "Illumination for computer generated pictures," *Commun. ACM*, vol. 18, pp. 311–317, June 1975.
- [8] G. J. Ward, "Measuring and modeling anisotropic reflection," *SIGGRAPH Comput. Graph.*, vol. 26, pp. 265–272, July 1992.
- [9] E. P. F. Lafortune, S.-C. Foo, K. E. Torrance, and D. P. Greenberg, "Non-linear approximation of reflectance functions," in *Proceedings of the 24th Annual Conference on Computer Graphics and Interactive Techniques, SIGGRAPH '97*, (New York, NY, USA), pp. 117–126, ACM Press/Addison-Wesley Publishing Co., 1997.
- [10] A. Sole, I. Farup, and S. Tominaga, "An image based multi-angle method for estimating reflection geometries of flexible objects," *Color and Imaging Conference*, vol. 2014, pp. 91–96, November 2014-11-03T00:00:00.
- [11] A. Sole, I. Farup, and S. Tominaga, "Image based reflectance measurement based on camera spectral sensitivities," *Electronic Imaging*, vol. 2016, no. 9, pp. 1–8, 2016.
- [12] J. A. Nelder and R. Mead, "A simplex method for function minimization," *The Computer Journal*, vol. 7, pp. 308 – 313, January 1965.

[13] CIE15.2, "Colorimetry." CIE standard, 2004.

## **Author Biography**

*Aditya Sole completed his bachelors from PVGs College of Engineering and Technology, Pune University, India in year 2005. In 2007 he completed his MSc in Digital Colour Imaging from London College of Communication, University of the Arts, London, UK. From 2008 till 2012 he worked as a Laboratory Engineer at the Norwegian Colour and Visual Computing Laboratory, Gjøvik University College, Gjøvik, Norway. Since, 2012 he is working as a Project Manager and is a PhD student at the Norwegian Colour and Visual Computing.*